COBEM 2023 27TH INTERNATIONAL CONGRESS OF MECHANICAL ENGENEERING

ABCM Brazilian Society of Mechanical Sciences and Engineering
27th ABCM International Congress of Mechanical Engineering
December 04-08, 2023, Florianópolis-SC, Brazil

COB-2023-0050
Nonlinear dynamics of a cantilever beam excited by a limited power supply with magnetic interaction

Eduardo Abuhamad Petrocino
José Manoel Balthazar
São Paulo State University. Av. Eng. Luiz Ed. C. Coube 14-01, Bauru-SP, ZIP:17033-360, Brazil
abuhamad@hotmail.com, eduardo.petrocino@unesp.br, jmbaltha@gmail.com, jose-balthazar@unesp.br

Marcos Silveira
Paulo José Paupitz Gonçalvez
São Paulo State University. Av. Eng. Luiz Ed. C. Coube 14-01, Bauru-SP, ZIP:17033-360, Brazil
marcos.silveira@unesp.br, paulo.paupitz@unesp.br

Ângelo Marcelo Tusset
Maurício Aparecido Ribeiro
Paraná Federal University. R. Dr. Washington S. Chuleire 330, Ponta Grossa-PR, ZIP:84017-220, Brazil
a.m.tusset@gmail.com, mau.ap.ribeiro@gmail.com

Leandro Rodrigo Oliveira
São Paulo State University. Av. Eng. Luiz Ed. C. Coube 14-01, Bauru-SP, ZIP:17033-360, Brazil
leandro.r.oliveira@unesp.br

Abstract. *Flexible structures with coupled motors, used in transporting materials and people, especially in industries, deserve attention, so that possible unwanted effects cause material damage and insecurity for people. A structure built with a cantilever beam with a motor with an unbalanced mass on its axis at its free end was used as the object of study in this article. Parametric excitation occurs in the beam, when the rotation of the motor axis increases, in a certain interval, it will cross its natural frequency, where the vibration is captured, increasing its amplitude, keeping its frequency constant until the moment of jump, a phenomenon known as the Sommerfeld effect, studied in energy systems with limited power. A passive way of reducing this effect without changing the properties of the beam material was proposed in this work, installing a permanent magnet on the free end of the beam, which will move inside with a resistance and a short-circuited coil. An induced current develops a magnetic field that will oppose the movement. As it is a dynamic system with slow oscillatory variations, an analytical modeling using the averaging theory was developed to estimate the dynamic behavior to compare with numerical simulations of the model and with the laboratory experiment. The acceleration of the beam, the current consumed by the dc motor and the angular speed of the motor shaft with the coil open, with a resistance and short-circuited were monitored. The system developed the predicted effects, and the magnetic interaction caused a perceptible reduction in the amplitude and time interval of the Sommerfeld effect.*

Keywords: *Non-linear dynamics, Cantilever beam, Limited power supply, Magnetic interaction ....*

1. INTRODUCTION

The study of dynamic systems excited by a limited energy source has been emerging in the field of engineering to overcome possible unwanted effects. A set of energy sources with limited power influenced by the vibrations of the structure is called a non-ideal energy system Kononenko (1969). A typical example of a non-ideal system is a motor with limited power coupled in a flexible structure, having an unbalance in its axis. In engineering, a turbine on an airplane wing or wind power generators, a gantry crane, among others, can serve as motivating examples for this study.

This type of problem, whose first record was made by the Swedish engineer C. G. P. de Laval, reported in Balthazar *et al.* (2003), where a turbine, when exceeding the natural frequency of the set, had reduced vibration amplitudes. This phenomenon of resonance capture and frequency hopping was studied by Arnold Sommerfeld Sommerfeld (1902), whose phenomenon is named after him. Kononenko (1969) made a profound study of non-ideal systems, and in his analyzes he used the average method, developed by Krylov and Bogoliubov (1947) and improved by Mitropolsky (1965). This method was applied in studies of relevant non-ideal systems such as Sanders *et al.* (2007); Nayfeh and Mook (2008); Balthazar (2022).

In this work, the proposed model is a beam fixed at one end, with a dc motor coupled to the free end. This system was

chosen because it is easily modeled and built, with modeling examples in Felix and Balthazar (2009), Gonçalves *et al.* (2014). Together with the dc motor, a magnet was fixed and immersed in the core of a coil, as done in Kuhnert (2020), which used reactive circuits at the coil terminals to promote vibration damping. In this article, the coil will have at its terminals only three different situations: open-circuit, with a resistance and in short-circuit.

The analysis is demonstrated with the motor rotation velocity starting statically up to the maximum rotation, passing through the natural frequency of the system, with the Sommerfeld effect occurring, where the frequency jump occurs, in which it escapes capture by resonance.

2. SYSTEM MODELING

A physical model can be represented as Fig. 1

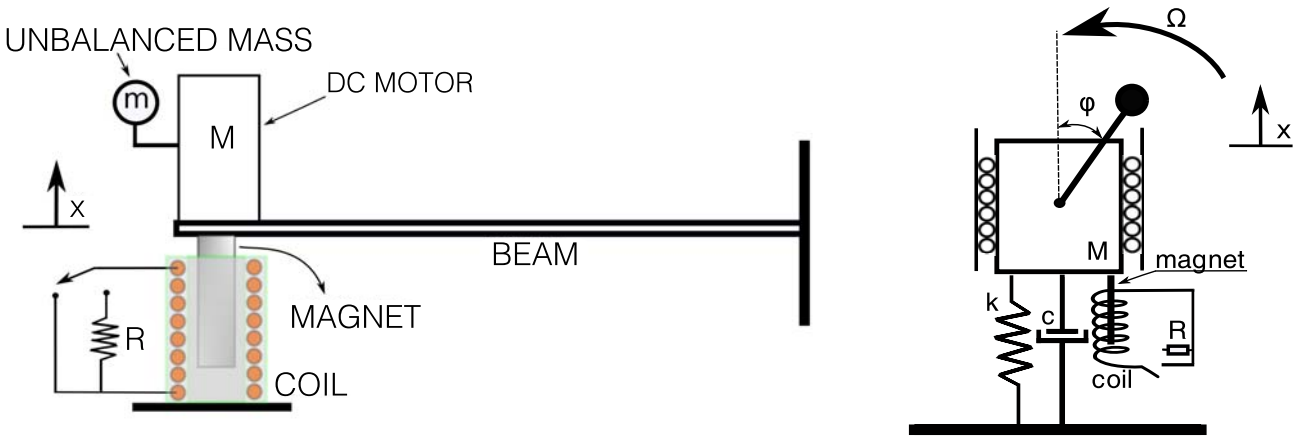

(a) (b)

Figure 1: Representation of the simplified structure (a) and the physical model for the first mode (b)

where M is the concentrated mass of the beam and motor, the unbalanced motor shaft is represented by a small mass m at a distance r from its center. The beam stiffness is represented by k and the damping coefficient is c. The electromagnetic set is represented by the circuit with the induced electromotive force, the ohmic resistance R, and by the ideal coil L coupled to the damping system.

2.1 Governing Equations of Motion

Considering J_0 the moment of inertia of the rotor, φ the angular position of the shaft, x the vertical position of the car, r the distance of the unbalanced mass to the center of the shaft, L the inductance of the coil and $\dot{Q}$ the electric current, expression of the kinetic energy T is obtained

$$T = \frac{1}{2}(M+m)\dot{x}^2 + \frac{1}{2}(J_0 + mr^2)\varphi^2 + mr\dot{x}\dot{\varphi}\sin\varphi + \frac{1}{2}\mathsf{L}\dot{Q}^2 \tag{1}$$

The potential energy U is

$$U = \frac{1}{2}kx^2 + \frac{1}{2}B\ell\dot{Q}x \tag{2}$$

where k is the spring constant, B is the magnetic induction modulus, and ℓ is the coil length.

The Lagrange equations have the form

$$\begin{aligned}
&\frac{d}{dt}\left(\frac{\partial\mathcal{L}}{\partial\dot{x}}\right) - \frac{\partial\mathcal{L}}{\partial x} = -c\dot{x} \\
&\frac{d}{dt}\left(\frac{\partial\mathcal{L}}{\partial\dot{\varphi}}\right) - \frac{\partial\mathcal{L}}{\partial\varphi} = L(\dot{\varphi}) - H(\dot{\varphi}) \\
&\frac{d}{dt}\left(\frac{\partial\mathcal{L}}{\partial\dot{Q}}\right) - \frac{\partial\mathcal{L}}{\partial Q} = -R\dot{Q}
\end{aligned} \tag{3}$$

The terms $L(\dot{\varphi})$ and $H(\dot{\varphi})$ represent the drive torque and the resistive torque of the system respectively. The Lagrangian being $\mathcal{L} = T - U$, substituting into Eq.(**??**), considering $\beta = B\ell$, $\mathfrak{M}(\dot{\varphi}) = L(\dot{\varphi}) - H(\dot{\varphi})$ and V as the potential difference applied to the electromagnetic circuit, the equations of motion are obtained

$$
\begin{aligned}
&(M+m)\ddot{x} + c\dot{x} + kx - \beta\dot{Q} = mr(\ddot{\varphi}\sin\varphi + \dot{\varphi}^2\cos\varphi)\\
&(J_0 + mr^2)\ddot{\varphi} = \ddot{x}mr\sin\varphi + \mathfrak{M}(\dot{\varphi})\\
&\mathsf{L}\ddot{Q} + R\dot{Q} + \beta\dot{x} = V
\end{aligned}
\tag{4}
$$

3. APPROXIMATE ANALYTICAL SOLUTION

To perform the Averaging Method, it is convenient to rewrite the equation in the form of Eq.(5) due to a small pertubative parameter ϵ. This parameter will be in first order, since only slow variations are analyzed, for other time scales it would be necessary to use the Multiple Scales Method

$$
\begin{aligned}
&\ddot{x} + \omega^2 x = \epsilon(q_2\ddot{\varphi}\sin\varphi + q_2\dot{\varphi}^2\cos(\varphi) - h\dot{x} + q_4 g\dot{x})\\
&\ddot{\varphi} = \epsilon(q_3\ddot{x}\sin(\varphi) + \mathfrak{M})\\
&\ddot{Q} = \epsilon(q_7 - q_5 g\dot{x} - q_6\dot{x})
\end{aligned}
\tag{5}
$$

where
$\omega^2 = \frac{k}{m+M}$; $\epsilon q_2 = \frac{mr}{m+M}$; $\epsilon q_3 = \frac{mr}{J}$; $\epsilon h = \frac{c}{m+M}$; $\epsilon q_4 = \frac{\beta}{m+M}$; $\epsilon q_5 = \frac{R}{L_i}$; $\epsilon q_6 = \frac{\beta}{L_i}$;
$\epsilon q_7 = \frac{V}{L_i}$; $\epsilon\mathfrak{M} = \frac{\mathfrak{M}(\dot{\varphi})}{J}$; $\dot{Q} = -\frac{\beta}{R}\dot{x}$; $g = -\frac{\beta}{R}$.

The new variables have slow variation as a function of time, A is the oscillation amplitude, Ξ the angular phase shift between x and the excitation force and θ the angular velocity of the shaft rotation of the engine, so it is convenient to write them

$$
x = A\cos(\varphi + \Xi);\ \frac{dx}{dt} = -A\omega\sin(\varphi + \Xi);\ \dot{Q} = -gA\omega\sin(\varphi + \Xi);\ \frac{d\varphi}{dt} = \theta
\tag{6}
$$

Solving the terms of the system of equations for the derivatives $\frac{dA}{dt}$, $\frac{d\Xi}{dt}$, $\frac{d\theta}{dt}$ and $\frac{dI}{dt}$, considering the first order terms of ϵ, the system of equations in standard form is obtained

$$
\begin{aligned}
&\frac{d\theta}{dt} = \epsilon\left[\mathfrak{M}(\theta) - q_3\theta A\omega\cos(\varphi + \Xi)\sin(\varphi)\right]\\
&\frac{dA}{dt} = -\frac{\epsilon}{\omega}\left[(hA\omega + \epsilon g\omega q_4 A)\sin(\varphi + \Xi) + q_2\cos(\varphi)\theta^2\right]\sin(\varphi + \Xi)\\
&\frac{d\Xi}{dt} = \epsilon\left\{\alpha_0 - \frac{1}{A\omega}\left[(\epsilon hA\omega + \epsilon g\omega q_4 A)\ sin(\varphi + \Xi) + q_2\cos(\varphi)\theta^2\right]\cos(\varphi + \Xi)\right\}\\
&\frac{dI}{dt} = \epsilon\left[q_7 + q_5 gA\omega\sin(\varphi + \Xi) + q_6 A\omega\sin(\varphi + \Xi)\right]
\end{aligned}
\tag{7}
$$

Perturbation is applied in the form $\varphi = \Omega t + \epsilon\Phi(t)$ where $\epsilon\Phi(t)$ is a small periodic function of t.

$$
\theta = \Omega + \epsilon U_1(t, \Omega, a, \xi);\quad A = a + \epsilon U_2(t, \Omega, a, \xi);\quad \Xi = \xi + \epsilon U_3(t, \Omega, a, \xi)
\tag{8}
$$

After performing the average, the system is obtained according to Eq.(9)

$$
\begin{aligned}
&\frac{d\Omega}{dt} = \epsilon\left(\mathfrak{M}(\Omega) + \frac{1}{2}q_3\omega a\Omega\sin(\xi)\right)\\
&\frac{da}{dt} = -\frac{\epsilon}{2}\left(ha + agq_4 + \frac{q_2\Omega^2\sin(\xi)}{\omega}\right)\\
&\frac{d\xi}{dt} = \epsilon\left(\alpha - \frac{\Omega^2 q_2\cos(\xi)}{2a\omega}\right)\\
&\frac{dI}{dt} = \epsilon q_7
\end{aligned}
\tag{9}
$$

The necessary conditions for the existence of stationary motions are equating the terms of Eq.(9) equal to zero for $\Omega \neq 0$:.

$$\begin{aligned}
&\mathfrak{M}(\Omega) + \frac{1}{2} q_3 \omega a \Omega \sin(\xi) = 0 \\
&ha + agq_4 + \frac{q_2 \Omega^2 \sin(\xi)}{\omega} = 0 \\
&\omega - \Omega - \frac{\Omega^2 q_2 \cos(\xi)}{2a\omega} = 0 \\
&q_7 = 0
\end{aligned} \tag{10}$$

Substituting the auxiliary variables, the oscillation amplitude equation is then obtained.

$$a = \frac{\Omega^2 mr}{\omega \sqrt{4m_0^2(\omega - \Omega)^2 + (\beta g + c)^2}} \tag{11}$$

The expression of the oscillation phase is

$$\tan(\xi) = \frac{\beta g - c}{2m_0(\Omega - \omega)} \tag{12}$$

To verify the curves, the parameters according to table 1 were used, inspired by the values of the items involved in the experiment.

Table 1: Beam parameters with motor and magnet

Parameter description	**Symbology**	**Value**	**Unit**
Young's modulus of beam	E	210×10^9	N/m
Beam density	ρ	8500	kg/m^3
Beam Width	b	25×10^{-3}	m
Beam thickness	h	1.5×10^{-3}	m
Cross-sectional area of beam	S	3.45×10^{-5}	m^2
Beam Length	l	9.9×10^{-2}	m
Magnet mass	m_i	63.8×10^{-3}	kg
Equivalent damping coefficient	c	0.2	Ns/m
Equivalent mass of the first way	M	120.3×10^{-3}	kg
Equivalent stiffness of the first mode	k	3.7117×10^3	N/m
Engine mass	M	25.1×10^{-3}	kg
Motor imbalance mass	m	4.8×10^{-3}	kg
Unbalance distance	r	0.02	m
Moment of Inertia	J_0	8×10^{-6}	Nm^2
Motor constant	k_t	11.46×10^{-3}	Nm/A
Armature Resistance	Ra	33.6	Ω
Maximum armature stress	va	5	V
Coil transductance parameter	β	59	Wb/m
Coil inductance	L	10.8	H
External voltage source on coil	V	0	V
Total electrical resistance in the coil	R	$variable$	Ω

In order to conclude the approximate solution of steady-state motion, it remains to obtain the terms $\epsilon U_1(t, \Omega, a, \xi)$, $\epsilon U_2(t, \Omega, a, \xi)$ and $\epsilon U_3(t, \Omega, a, \xi)$ from Eq.(8). θ, A and Ξ will be replaced by the approximate values Ω, a and ξ in Eq.(7).

Eq.(8) can be rewritten

$$\begin{aligned}
&\frac{d\varphi}{dt} = \Omega + \frac{mra\omega}{4J} \cos(2\Omega t + \xi) \\
&A = a + \frac{1}{4}\left[\frac{\Omega mr}{(M+m)\omega} \cos(2\Omega t + \xi) + \frac{a(c - \frac{\beta^2}{R}) \sin(2(\Omega t + \xi))}{2(M+m)}\right] \\
&\Xi = \xi - \frac{1}{4}\left[\frac{\Omega mr}{(M+m)a\omega} \sin(2\Omega t + \xi) - \frac{(c + \frac{\beta^2}{R}) \cos(2\Omega t + \xi)}{2(M+m)}\right]
\end{aligned} \tag{13}$$

Reversing the variables x and dx/dt given in Eq.(6) we have the approximate solution equation

$$x = a\cos(\Omega t + \xi) + \frac{\Omega m r}{4\omega(M+m)}\left(1 - \frac{(M+m)\omega^2 a^2}{2J_0\Omega^2}\right)\cos(\Omega t) \tag{14}$$
$$+\frac{a(c+\frac{\beta^2}{R})}{4\Omega(M+m)}\sin(\Omega t+\xi) + \frac{mr\omega a^2}{8J_0\Omega}\cos(3\Omega t + 2\xi)$$

In this way, the temporal history is obtained by increasing the rotation frequency, as seen in Figure 2. This figure represents the amplitude variations with the increase of the signal frequency as a function of time. There is a stronger increase in amplitude from 120 seconds onwards, at which point there is resonance capture. There are no frequency jumps, as only stationary movements were considered.

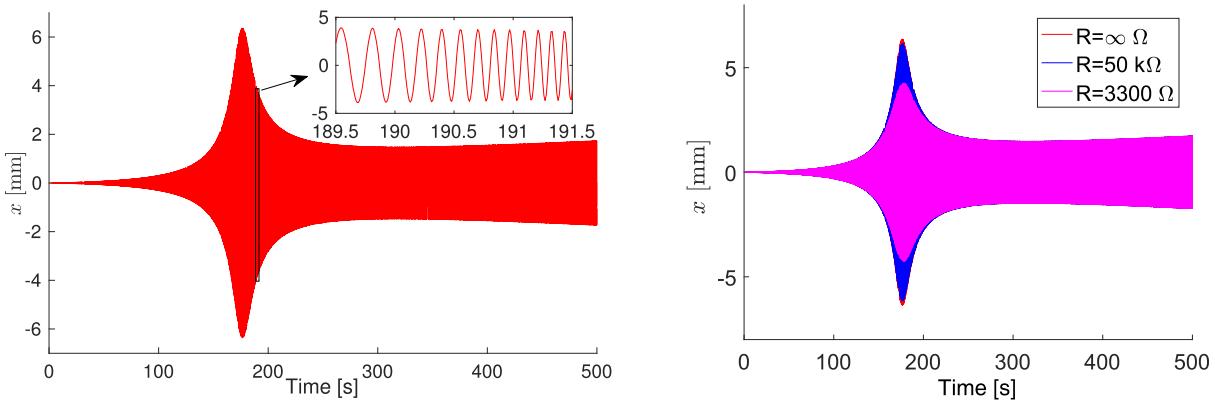

(a) Waveform details at a 2s interval

(b) Oscillogram with resistance variations

Figure 2: Graphics of time history of oscillation amplitude as a function of time in seconds

Integrating the Eq.(9), using the Matlab numerical computation application, with relative and absolute error tolerance values of $1 \cdot 10^{-10}$, initial step size and final step size of integration respectively of $1 \cdot 10^{-12}$ and $1 \cdot 10^{-3}$, from adopted initial conditions, one obtains the non-stationary conditions when passing through the resonance shown in the Figure 3. In Figure 3b it is possible to observe the capture by resonance at 28Hz and the frequency jump, whose time interval depends on the magnetic damping.

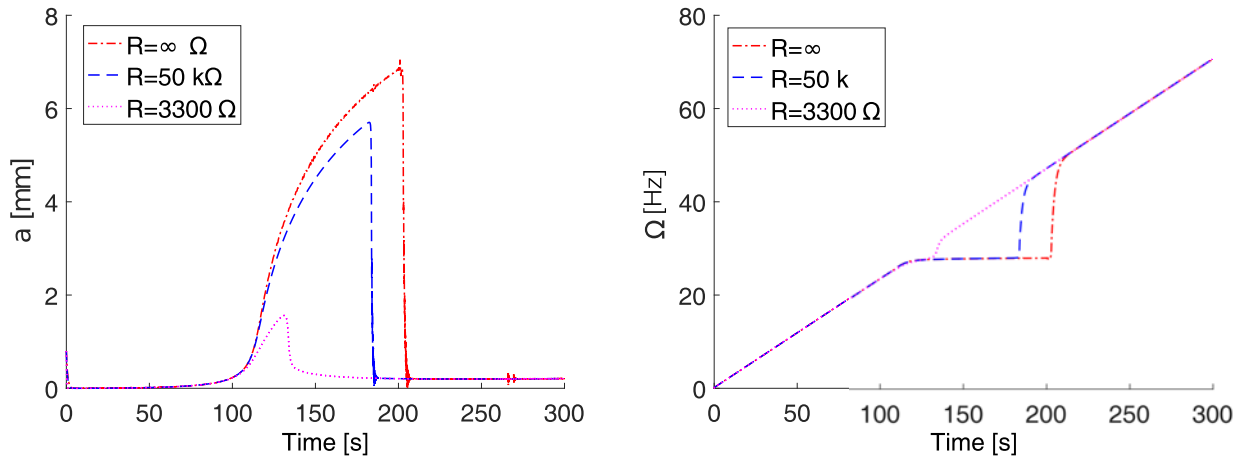

(a) Amplitude envelope

(b) Angular speed

Figure 3: Graphics of non-stationary movements with increasing frequency as a function of time in seconds with the three resistance values

4. NUMERICAL SOLUTION

The naming of the variables from previous chapters is maintained, x is the vertical displacement of the structure, φ is the angular position of the motor shaft and q is the electrical load. For system-order reduction, rewrite the state variables

of Eq.(4), adopting $y_1 = x$, $y_2 = \dot{x}$, $y_3 = \varphi$, $y_4 = \dot{\varphi}$, $y_5 = q$ and $y_6 = \dot{q}$, as follows:

$$\begin{aligned} \dot{y}_1 &= y_2 \\ \dot{y}_3 &= y_4 \\ \dot{y}_5 &= y_6 \end{aligned} \tag{15}$$

The matrix form of the accelerations is obtained

$$\begin{bmatrix} M+mr & -mr\sin(y_3) & 0 \\ -mr\sin(y_3) & mr^2+J0 & 0 \\ 0 & 0 & L \end{bmatrix} \begin{bmatrix} \dot{y}_2 \\ \dot{y}_4 \\ \dot{y}_6 \end{bmatrix} = \begin{bmatrix} -cy_2 - kx + mr\cos(y_3)y_4^2 r + By_6 \\ \mathfrak{M}(y_4) \\ -By_2 - Ry_6 + V \end{bmatrix} \tag{16}$$

Inverting the matrix on the left side and multiplying by the matrix on the right side in Eq.(16), one obtains the state equations in Eq.(17) suitable for using the computational method of integration

$$\begin{aligned} \dot{y}_2 &= \frac{L(mr^2+J_0)(-cy_2 - kx + m\cos(y_3)y_4^2 r + \beta y_6) + Lm\mathfrak{M}(y_4)\, sin(y_3) r}{L(m+M)(mr^2+J_0) - Lm^2\sin(y_3)^2 r^2} \\ \dot{y}_4 &= \frac{Lm\sin(y_3)r(-cy_2 - kx + m\cos(y_3)y_4^2 r + \beta y_6) + L(m+M)\mathfrak{M}(y_4)}{L(m+M)(mr^2+J_0) - Lm^2\sin(y_3)^2 r^2} \\ \dot{y}_6 &= \frac{\left((m+M)(mr^2+J_0) - m^2\sin(y_3)^2 r^2\right)(-\beta y_2 - Ry_6 + V)}{L(m+M)(mr^2+J_0) - Lm^2\sin(y_3)^2 r^2} \end{aligned} \tag{17}$$

Numerical simulations are done with the ODE45 command, which is a solver integrated in the MATLAB library that uses a variable step technique based on the Dormand and Prince (1980) method. The simulations were performed with relative and absolute error tolerance values are $1 \cdot 10^{-10}$, initial step size and maximum integration step size respectively $1 \cdot 10^{-12}$ and $1\ cdot 10^{-3}$. The initial values will be considered zero for all variables, the results are presented with three resistance values of the electromagnetic circuit, open circuit $R = \infty$, with total resistance of 50 $k\Omega$ and with total resistance of 3300 Ω.

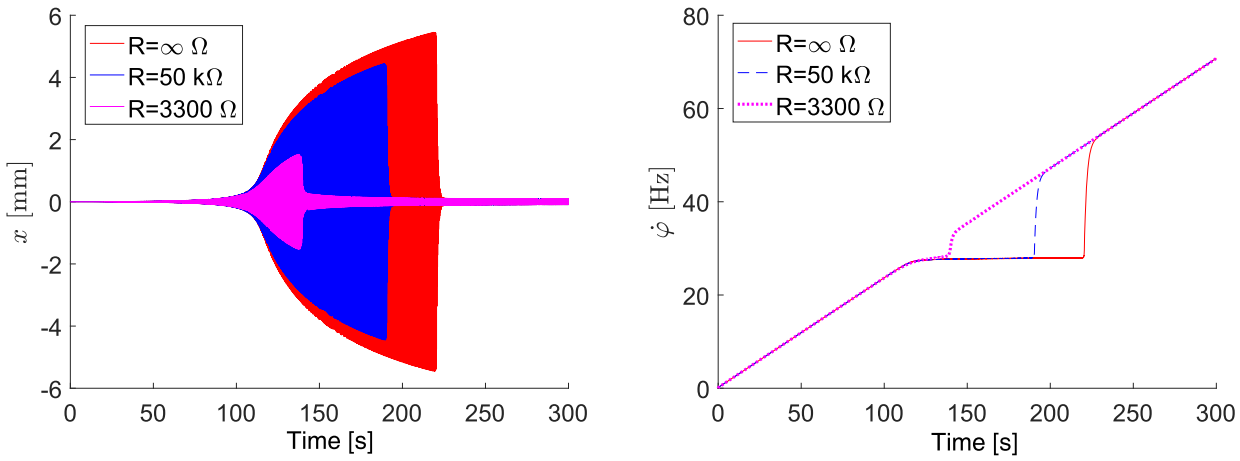

(a) Structure offset

(b) Angular speed

Figure 4: Graphs resulting from numerical simulations (a) speed, (b) displacement, (c) frequency and (d) current in the coil, all as a function of time in seconds, with increasing frequency direction and with different resistance values

The losses in the motor were not considered, the beam was considered with homogeneous and isometric density, and any non-linearities that could compose the dynamics of the beam, the electrodynamics in the conductors and the magnetic interaction of the structure with the coil were also neglected.

5. EXPERIMENTAL RESULTS

The experimental tests were carried out at the Laboratory of Acoustics and Vibration of the São Paulo State University. The set is formed by a wooden base for fixing and supporting the test elements, the base is on an inertial table without additional fixation, only with its weight, a stainless steel beam with the specifications described in the Table 1. The complete system is shown in Figure 5, it can be seen that the permanent magnet is almost entirely immersed in the coil core. The coil was wound on a printed support in the laboratory, it has 27000 turns, resulting in an inductance of 10.8 H.

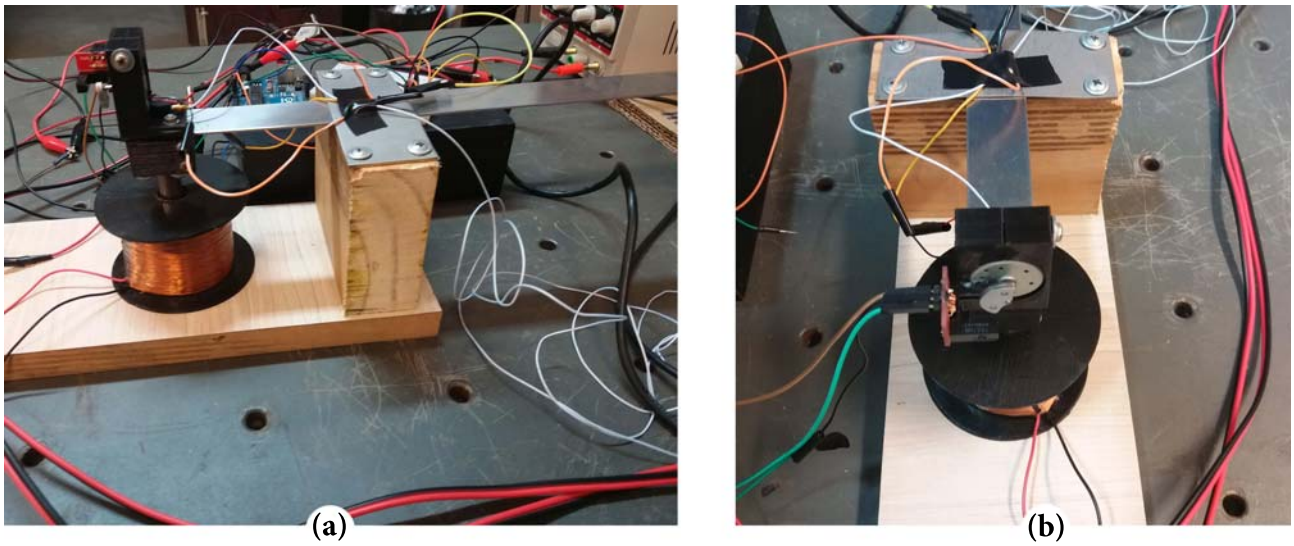

Figure 5: System photo (a) side and (b) front

The PWM output has an average voltage amplitude in the range of 0 to 5 V, the treatment of values is done in percentage of the work cycle time, “Duty Cycle”, of the PWM signal, where the amplitude of 5 V corresponds to 100%. The range used in this experiment is from 18% to 60%, with steps of 0.8%, the duration of each step is 5 s, resulting in each series of measurements 53 steps performed in 265 seconds.

The data acquisition equipment is the National Instruments, model USB-4431, which has four simultaneous data input. The first input is used to monitor an accelerometer from PCB Piezotronics, model 352A59, the second input monitors the voltage produced in the coil, the third input monitors the voltage applied to the motor and the fourth input monitors the optical switch, tests were carried out on several batteries to include the measurement of the electric current consumed by the motor indirectly.

The set of sensors, signal processing and PWM actuator can be seen in general in Figure 6.

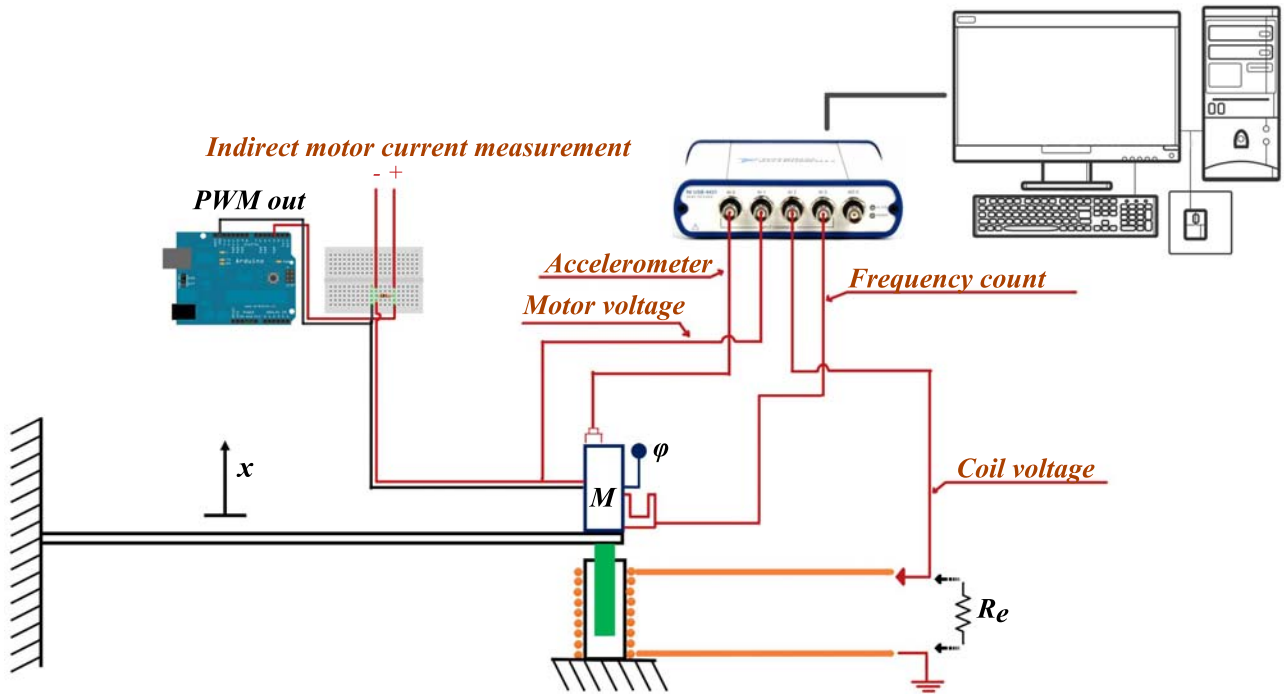

Figure 6: Test bench

The monitoring of the motor allowed producing the graph of the power consumed as a function of the rotation speed of its shaft, shown in Fig 7a. The waveform generated by the accelerometer, with the details shown in Fig. 7b.

The accelerations as a function of time for many resistors with increasing voltage applied to the motor are presented in Figure 8a, it is noticed that each graph with its respective resistance coupled, starts practically at the same instant , having

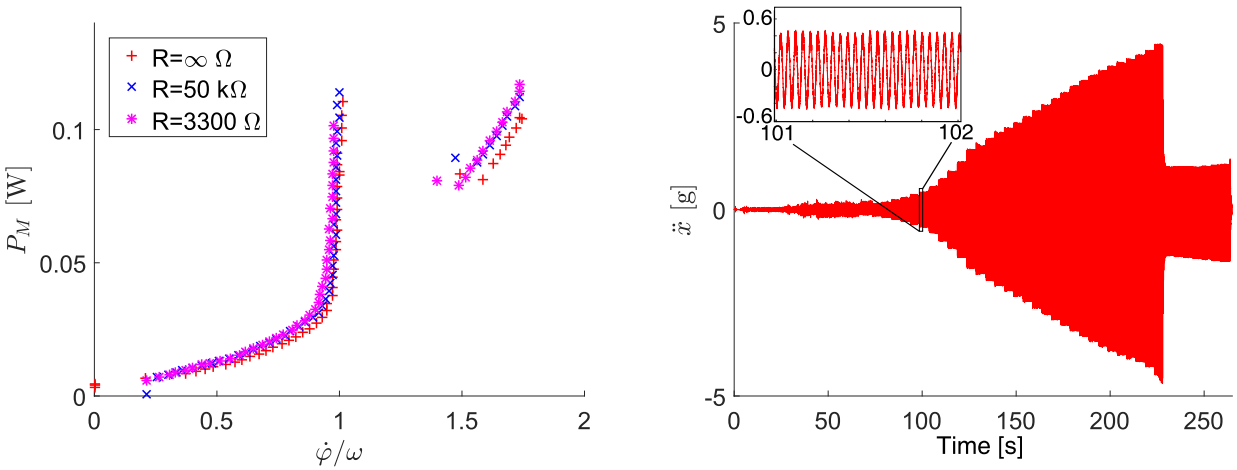

(a) (b)

Figure 7: Graphics of the monitoring of the (a) motor power as a function of normalized frequency and (b) the acceleration as a function of time in seconds, with waveform detail.

the jump, at the end of the capture, determined by the resistance value. The time histories of the frequencies, with the resistance variations and with the increasing voltage applied to the motor, in this graph, shown in Figure 8b, it can be seen that the natural frequency of the system where the resonance capture occurs is around 28 Hz.

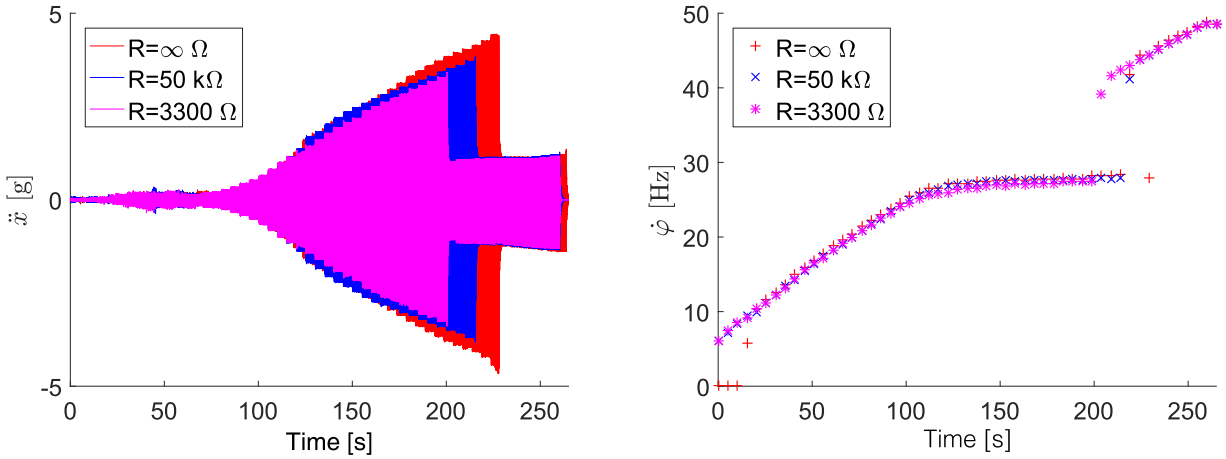

(a) Acceleration as a function of time (b) Rotor frequency as a function of time

Figure 8: Monitoring the behavior of the structure with increasing voltage and changing resistances as a function of time in seconds

6. FINAL CONSIDERATIONS

To demonstrate the effectiveness of the dynamic damper as a function of different currents controlled by purposely added external resistances, the study is carried out close to the resonant frequency, since the phenomena that occur in this spectrum range offer a non-linear response, behavior caused by the Sommerfeld effect .

Approximate analytical solutions, solutions resulting from numerical simulations and experimentally obtained data were described.

Initially, the oscillation amplitude of the structure during the observation interval is compared. For the analytical solution, the envelope obtained by integrating the equation of motion in non-stationary amplitude is used, for the numerical solution, the waveform obtained from successive numerical integrations is used for the displacement in x, and for the experimental solution, the acquired waveform, with double integration. For a better exposition, the amplitude results were superimposed as a function of time and shown in Figure 9a.

There is a little noise in the experimental result, actually a subharmonic, but the reading is not affected. Another point to be considered in the experimentally measured wave is the discretization, which occurred in the voltage applied to the

armature in small steps caused by the PWM resolution, giving the appearance of steps. The waveforms are very similar to each other, in addition to the aforementioned amplitude, the engine speed is displayed as a function of time in Figure 9b. It is shown that the frequency hopping amplitudes present some differences, caused by neglected nonlinearities in the experimental apparatus, however the damping effect is consistent in all forms.

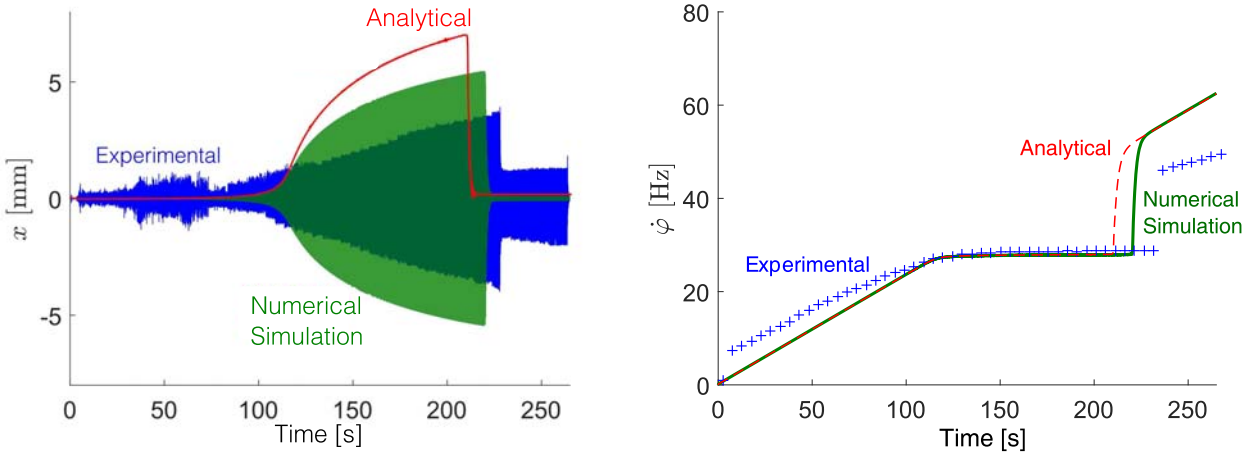

(a) Comparison between amplitudes

(b) Comparison between the angular speeds of the motor shaft

Figure 9: Comparison of results obtained for amplitude (a) and frequency (b) as a function of time, between analytical, numerical and experimental solutions, for the direction of increasing frequency.

The time histories of the results of numerical and experimental simulations have great similarities in waveforms and values, both for acceleration and for the angular velocity of the motor shaft. The Sommerfeld effect was well exposed, and through this effect it is possible to verify the performance of the electromagnetic circuit, reducing the amplitude of oscillation of the beam and reducing the size of the jump in frequency.

7. ACKNOWLEDGEMENTS

We thank professors Dr. Paulo J.P. Gonçalves and Dr. Marcos Silveira for authorizing the use of the laboratory and data acquisition and processing equipment of the Department of Mechanical Engineering.

8. REFERENCES

Balthazar, J.M., 2022. *Nonlinear Vibrations Excited by Limited Power Sources*. Springer, Springer International Publishing.

Balthazar, J.M., Mook, D.T., Weber, H.I., Fenili, A., Belato, D. and Felix, J., 2003. "An overview on non-ideal vibrations". *Meccanica*, Vol. 38, pp. 613–621.

Dormand, J.R. and Prince, P.J., 1980. "A family of embedded runge-kutta formulae". *Journal of computational and applied mathematics*, Vol. 6, No. 1, pp. 19–26.

Felix, J.L.P. and Balthazar, J.M., 2009. "Comments on a nonlinear and nonideal electromechanical damping vibration absorber, sommerfeld effect and energy transfer". *Nonlinear Dynamics*, Vol. 55, No. 1, pp. 1–11.

Gonçalves, P., Silveira, M., Junior, B.P. and Balthazar, J., 2014. "The dynamic behavior of a cantilever beam coupled to a non-ideal unbalanced motor through numerical and experimental analysis". *Journal of Sound and Vibration*, Vol. 333, No. 20, pp. 5115–5129.

Kononenko, V.O., 1969. *Vibrating systems with a limited power supply*. Iliffe.

Krylov, N.M. and Bogoliubov, N.N., 1947. *Introduction to Non-Linear Mechanics.(AM-11), Volume 11*. Princeton university press.

Kuhnert, W.M., 2020. "On the design of electromechanical vibration isolators and energy harvesters".

Nayfeh, A.H. and Mook, D.T., 2008. *Nonlinear oscillations*. John Wiley & Sons.

Sanders, J.A., Verhulst, F. and Murdock, J., 2007. *Averaging methods in nonlinear dynamical systems*, Vol. 59. Springer.

Sommerfeld, A., 1902. "Beiträge zum dynamischen ausbau der festigkeitslehe". *Physikal Zeitschr*, Vol. 3, pp. 266–286.

9. RESPONSIBILITY NOTICE

The following text, properly adapted to the number of authors, must be included in the last section of the paper: The author(s) is (are) solely responsible for the printed material included in this paper.